AD-A110 822 PITTSBURGH UNIV PA DEPT OF CHEMISTRY F/G 7/4
LASER DESORPTION MASS SPECTROMETRY. II. APPLICATIONS TO STRUCTU--ETC(U)
FEB 82 D M HERCULES, R J DAY, K BALASANMUGAM N00014-81-K-0408
UNCLASSIFIED TR-1 NL

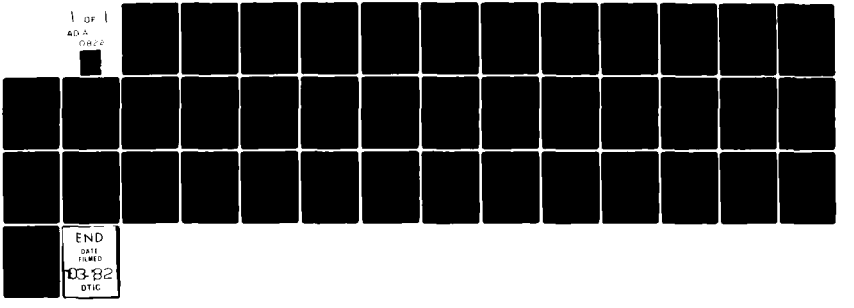

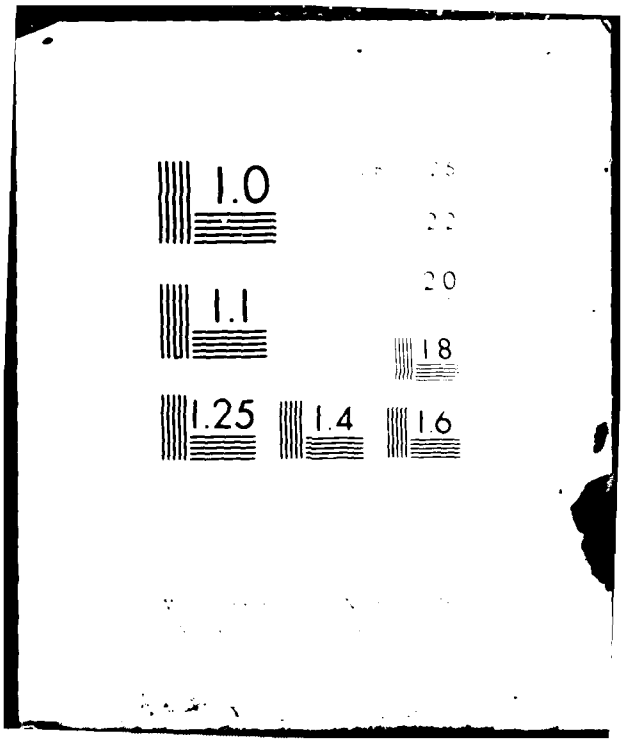
1.0
1.1
1.25
1.4
1.6
18
20
22

LEVEL II

12

OFFICE OF NAVAL RESEARCH

Contract Number N00014-81-K-0408

Task Number NR 051-774/5-29-81[472]

TECHNICAL REPORT NO. 1

AD A110822

Laser Desorption Mass Spectrometry. II.

Applications to Structural Analysis

by

David M. Hercules, R. J. Day, K. Balasanmugam,

Tuan A. Dang and C. P. Li

Prepared for Publication

in

Analytical Chemistry

University of Pittsburgh
Department of Chemistry
Pittsburgh, PA 15260

February 2, 1982

82 02

4

SECURITY CLASSIFICATION OF THIS PAGE (When Data Entered)

REPORT DOCUMENTATION PAGE		READ INSTRUCTIONS BEFORE COMPLETING FORM
1. REPORT NUMBER 1	2. GOVT ACCESSION NO. AD-A110 822	3. RECIPIENT'S CATALOG NUMBER
4. TITLE (and Subtitle) LASER DESORPTION MASS SPECTROMETRY. II. APPLICATIONS TO STRUCTURAL ANALYSIS		5. TYPE OF REPORT & PERIOD COVERED Interim Technical Report 6. PERFORMING ORG. REPORT NUMBER
7. AUTHOR(s) David M. Hercules, R. J. Day, K. Balasanmugam, Tuan A. Dang and C. P. Li		8. CONTRACT OR GRANT NUMBER(s) N00014-81-K-0408
9. PERFORMING ORGANIZATION NAME AND ADDRESS Department of Chemistry University of Pittsburgh Pittsburgh, PA 15260		10. PROGRAM ELEMENT, PROJECT, TASK AREA & WORK UNIT NUMBERS 051-774/5-29-81[472]
11. CONTROLLING OFFICE NAME AND ADDRESS Office of Research University of Pittsburgh, 200 Gardner Steel Bldg Pittsburgh, PA 15260		12. REPORT DATE February 2, 1982 13. NUMBER OF PAGES 38
14. MONITORING AGENCY NAME & ADDRESS(if different from Controlling Office)		15. SECURITY CLASS. (of this report) Unclassified 15a. DECLASSIFICATION/DOWNGRADING SCHEDULE

16. DISTRIBUTION STATEMENT (of this Report)

This document has been approved for public release and sale; its distribution is unlimited.

17. DISTRIBUTION STATEMENT (of the abstract entered in Block 20, if different from Report)

Same

18. SUPPLEMENTARY NOTES

Published in Analytical Chemistry , February 1982

19. KEY WORDS (Continue on reverse side if necessary and identify by block number)

Laser desorption mass spectrometry
nonvolatile organic compounds
Cationization reactions
Polymers
ion-molecule reactions
quantitative analysis

20. ABSTRACT (Continue on reverse side if necessary and identify by block number)

Laser desorption mass spectrometry (LDMS) is reviewed with focus on application to structural analysis of nonvolatile organic compounds. Models for the ionization-volatilization step are discussed with reference to solid-state vs. "gas-phase" reactions. General characteristics of LDMS of organic compounds are discussed; for example, classes of compounds that generate $M^{+\cdot}$ ions or $(M+H)^+$ ions. Cationization reactions are considered; organic salts are discussed. Particular emphasis is placed on LDMS of high molecular weight

DD FORM 1 JAN 73 1473 EDITION OF 1 NOV 65 IS OBSOLETE
S/N 0102-014-6601

Unclassified

SECURITY CLASSIFICATION OF THIS PAGE (When Data Entered)

20. compounds such as polysaccharides, polymers and vitamin B_{12} and its relatives. Problems of ion-molecule reactions complicating spectra are considered, particularly for transition metal coordination compounds. Other topics considered include quantitative analysis, microprobe applications and sample handling.

Introduction

Application of structural mass spectrometry to diverse materials (primarily organic compounds) has increased during the past several decades. There has been considerable interest in extending the technique to materials that are polymeric, have high molecular weight, low volatility, and/or are thermally unstable. Although derivatization has extended the scope of structural mass spectrometry to some materials that are not normally volatile, derivatization techniques are not universally applicable. Problems arise with functionalities not readily derivatized to produce volatile compounds, or from side reactions which complicate mass spectra. Thus, there has been considerable interest in obtaining mass spectra directly from solids without derivatization. Workers have applied a variety of ingenious methods to obtain mass spectra of solids and these have been summarized in a recent review (1). Thus only a few of the approaches will be mentioned here; those which are most important as a backdrop for discussion of laser mass spectrometry.

Attempts to obtain mass spectra of solids have used one of two general approaches: enhanced sample volatilization or direct ionization either from a surface or from the bulk solid. Much work in the former category involved modification of electron impact mass spectrometers to obtain spectra directly from solids. This has included use of in-beam heating methods, rapid heating, desorption, flash desorption, and spark sources. Similarly, desorption and in-beam heating techniques have been applied to chemical ionization mass spectrometry.

Development of field-desorption mass spectrometry (FDMS) (2) marked a milestone as the first generally applicable technique for ionization directly from a solid. Field desorption sources for conventional mass spectrometers have become widely used. However, despite all of its advantages, FDMS remains very much an art and obtaining high quality spectra frequently is tedious. Thus, although it has been very successful, FDMS is not optimum.

Several other mass spectrometric techniques have been applied to solids and although each has experienced some success, none is yet a routine method for the analysis of solids. One of the most promising techniques, plasma desorption, shows considerable potential for high molecular weight compounds, ions in excess of m/z 10,000 have been observed (3). Secondary ion mass spectrometry (SIMS) has been a useful technique for obtaining mass spectra of solids including amino acids, other organic molecules (4) and polymers (5). Fairly large molecules can be ionized by cation attachment during SIMS (6). The closely related fast atom bombardment technique (FAB) has generated outstanding results and intense interest (7).

Various laser systems have been used in mass spectrometer ion sources but in general, laser desorption has suffered from lack of speed and/or sensitivity, limited mass range or a combination of these factors (8,9). However, these earlier studies clearly demonstrated the potential of the laser desorption technique. Development of laser ionization mass spectrometry has been characterized by diversity. Various modes have been used, e.g. laser desorption and laser evaporation, coupled with various instrumental configurations. A recent review (10) has brought together much of the diverse research in a concise and effective manner.

Development of a commercial laser microprobe mass spectrometer (11) (Leybold-Heraeus LAMMA^{R}-500)* represents a significant breakthrough in laser mass spectrometry, particularly in its application to non-volatile organic compounds. The first report in this series (12) has discussed the instrument in detail. Also, the report dealt with an evaluation of the LAMMA-500 in regard to sample requirements, analysis time, ionization characteristics, speciation capabilities and interferences. The present report will deal with application of the LAMMA-500 to structural mass spectrometry. Much still remains to be learned about LD mass spectrometry, and the present article will focus on some examples (mostly from our laboratory) of its application to date. We will stress the diversity of systems that can be studied, presenting a perspective about the scope of potential applicability of the LAMMA-500.

Mechanism of Laser Ionization/Volatilization

The mechanism of ion formation from laser irradiation of solids is not well established. A recent review (13) has dealt with some aspects of this topic. It is generally conceded (10) that the wavelength of the laser is not an imporant parameter, although this conclusion has been established from studies on a limited number of systems. One of the most important parameters is the duration and shape of the laser pulse, which frequently has not been considered in wavelength dependence studies.

Although the time-profile of the laser pulse is a simple function and can be well-defined, the time profile of ion and atom emission is not.

*LAMMA^{R} is a registered trademark of Leybold-Heraeus GmbH.

This is because a variety of processes contribute to laser-induced emission from solids, including vaporization, shock waves and gas dynamics. The emission volume of a solid is probably best characterized as a fully ionized plasma.

Ionization efficiency, defined as the ratio of ions to neutrals created by the plasma, varies with laser power density (10). It appears that below power densities of 10^8 W/cm^2 ionization efficiency is approximately 10^{-5}. At power densities in the range 10^9 - 10^{10} W/cm^2, ionization efficiencies in the range 0.01 - 0.1 have been reported.

Another important factor is the variation of ionization efficiencies for different elements in the same matrix. Although there is not unanimity on this point, it appears from accumulated data that relative elemental sensitivity factors are reasonably constant as a function of both atomic number and laser power density, as long as one is dealing with the same matrix. These data were obtained using power densities (approximately 10^{10} W/cm^2) where single ionization phenomena dominate (10).

Models of Volatilization/Ionization - There are at least five processes to be considered when discussing volatilization/ionization by pulsed lasers: 1) direct ionization of the solid by the laser beam; 2) desorption and ionization of the solid in the region immediately adjacent to the laser pulse; 3) surface ionization; 4) gas-phase (ion-molecule) reactions; 5) emission of neutral particles vs. ion formation. Figure 1 outlines the importance of these phenomena to the laser ionization/volatilization process. Direct ionization by the laser must occur in the region impacted by the laser beam, λ. Although estimates of the temperature in this region vary, a temperature between 3000 and 6000°K seems to be

reasonable. Thus it is likely that only atomic ions and small molecular fragments are emitted directly from region 1. This is based on the assumption that this region operates sufficiently close to thermal equilibrium that the temperature measured is characteristic of the system.

Immediately adjacent to the region impacted by the laser will be a region of high thermal gradient (2), influenced by the shockwave from both the laser impact and from the collapsing plasma. It seems reasonable that higher molecular weight ions and neutrals will be emitted from this "cooler" region. Although region 2 is not at the temperature of the plasma, it is probable that solid state reactions occur in this region which are responsible for emission of ions. A topic of current debate in laser mass spectrometry concerns direct ionization in the solid vs. ion formation by "gas phase" reactions in the region immediately above the surface. According to the model of Fig. 1, surface ionization should occur in the region immediately adjacent to the laser beam, 3. Any "gas-phase" reactions will occur in the "cloud" over the impacted region (4) whether the ions formed by ion-molecule reactions are quasimolecular ions or cluster ions. Evidence seems to indicate that both solid state and "gas-phase" reactions occur, although the relative importance of the two processes is still in question.

The time-dependence of the processes in Figure 1 must be considered and should be useful for distinguishing between them. Ion desorption and emission of neutrals should not have the same time-profile as ions produced directly by the laser pulse. Qualitative time profiles of the various processes are shown in Figure 2. Ions produced directly in the region of the laser pulse (1) will be generated only while the laser

beam is incident on the sample· thus they will have essentially the same time profile as the laser pulse. Although ion emission from regions adjacent to the laser pulse will occur while the laser beam is incident on the sample, because these ions are generated by secondary effects, emission will continue after the laser pulse has been extinguished. Thus a "phase shift" will occur between these "secondary" ions and those from the laser pulse. Because ionization is a higher energy process than emission of neutrals, neutral emission will probably continue for some time after emission of ions from the sample has ceased.

Given the different time domains for ion production directly by the laser, "secondary" ion emission and emission of neutrals, it should be possible to separate the three phenomena. Ionization of neutrals using a CI source coupled to a laser mass spectrometer has been demonstrated (14). Laser desorption experiments using both magnetic and quadrupole instruments have also shown that particle emission continues after termination of the laser pulse.

Instrumentation

Laser induced ion sources have been used with a variety of mass analyzers and instrumental configurations. A host of lasers has been used having photon energies from the infrared to the ultraviolet, and pulse widths from picoseconds to continuous wave. Instruments also vary with respect to the angle between the incoming laser beam and the mass spectrometer axis (10).

Most LDMS systems have employed time-of-flight (TOF) mass spectrometers. TOF analyzers are ideally suited for obtaining mass spectra of solids following pulsed laser irradiation. Short ion formation time is necessary

for optimum mass resolution. A mass spectrum can be obtained for each laser pulse. This is not possible with scanning mass spectrometers. Although pulsed lasers are required in the case of TOF mass analysis, they need not be used when other analyzers are employed. A critical parameter, though, is laser power density, 10^6 - 10^{10} W/cm^2 being needed to generate a sufficient number of ions for a TOF to measure. LD mass spectra have been obtained with infra-red, visible and ultraviolet lasers. Mass spectra do not appear to vary as a function of wavelength.

Various geometries between the exciting beam and the mass spectrometer axis have been used. These can be divided into two classes: those in which the laser beam is transmitted through the sample as in the LAMMA-500, and those in using a front-surface mode. In the former case, samples must be thin enough for the laser beam to penetrate them. In the latter case, thick samples can be used, since the laser irradiates the mass spectrometer side of the material. An advantage of the transmitting geometry is use for microprobe analysis. Thin sections can be viewed through a microscope, the laser focused on a specific spot, and a mass spectrum obtained.

Details of the LAMMA-500 will not be discussed here because they have already been treated in the previous article in these pages (12).

Spectra of Organic Compounds

General Characteristics - For some compound classes, laser desorption generates odd-electron ions, similar to those observed in regular electron impact (EI) mass spectra. For example, LD mass spectra of polycyclic aromatic hydrocarbons are characterized by abundant molecular ions, $M^{+\cdot}$ in the positive ion spectrum (15). Radical ions are also generated for a

number of compounds containing heteroatoms in addition to aromatic functions. For example laser desorption of bis(dimethylamino)benzophenone, gives odd-electron molecular cations, at m/z 268 as shown in Figure 3 top. The M+1 peak is higher than would be expected from the ^{13}C isotope contribution, indicating some $(M+H)^+$ contribution. The peak at 268 is the only major peak higher than m/z 120. Similarly, $(M-H_2)^{-\cdot}$ dominates the negative ion LD mass spectrum of bianthrone as shown in Fig. 3 bottom. Again, it is the only major peak in the high-mass region. Molecular ions ($M^{+\cdot}$) of triphenylphosphine are emitted during laser irradiation at low power densities. At higher power densities the $(M+H)^+$ peak at m/z 263 dominates the spectrum, indicating competition between $M^{+\cdot}$ and $(M+H)^+$ formation. The $(M+77)^+$ peak at m/z 339 corresponds to an ion-molecule reaction, even at low power densities. A compound for which radical anion emission was unexpected, was the quaternary amine Safranin-O. Ions corresponding to $(M-HCl)^{-\cdot}$ at m/z 313 dominate the negative ion mass spectrum.

Two classes of positive quasimolecular ions are common in LD, protonated ions $(M+H)^+$, and cationized molecules $(M+C)^+$. For many compound classes, only cationized species are observed. Such varied compounds as ascorbic acid, atropine and glycocholic acid yield abundant $(M+H)^+$ ions in LD. Frequently $(M-H)^-$ ions are observed for compounds having acidic functional groups. An example of a compound having both strong $(M+H)^+$ and $(M-H)^-$, ions is asparagine, shown in Figure 4. It should be noted that only a few peaks are seen in both the positive- and negative-ion spectra of asparagine. The peak at m/z 87 in the positive spectrum corresponds to loss of formic acid from $(M+H)^+$, and the peak at m/z 44 probably corresponds to $CONH_2^+$.

In the negative-ion spectrum, the only significant fragment-ion peak (m/z 114) corresponds to loss of NH_3 from $(M-H)^-$. The peak at m/z 26 is due to CN^-, a common ion found in the negative spectrum of nitrogen-containing organic compounds. At higher power densities CN^- and C_3N^- can dominate the negative-ion LD spectra of nitrogen-containing compounds. Similarly, CNO^- is a common peak found in compounds containing carbon, nitrogen and oxygen.

Sometimes cationized molecules are observed along with $(M+H)^+$ as shown in Figure 5-top. In this case, the $(M+H)^+$ and $(M+Na)^+$ peaks for glycocholic acid are approximately equal in intensity. No sodium salt was added to the sample used for Fig. 5. Cationization frequently occurs with small amounts of Na impurities. In some cases $(M+C)^+$ ions (C = cations) are the only quasimolecular ions detected. For example, Figure 5 (bottom) shows the spectrum of stachyose obtained from a 5:1 stachyose NaCl mixture. Protonated carbohydrate molecules are not observed in LD but cationization is a common process. In addition to the $(M+Na)^+$ peak at 689, stachyose shows peaks at m/z 527 and 365 which correspond to cationized tri- and di-saccharide fragments, respectively.

Many metals can participate in cationization processes. For example, LD of sucrose has given rise to $(M+Na)^+$, $(M+K)^+$ and $(M+Ag)^+$ ions. We have observed cationization of several samples by Co, Cu, Pb, Cd and Li. Recent thermal desorption and LD chemical ionization experiments have suggested that cation attachment occurs by co-desorption of metal ions and neutral molecules (16). Thus, alkali ions produced by thermal emission would attach to neutral molecules desorbed in the same excitation event.

Anionization, attachment of an anion to an intact molecule, has been observed in FD, electrohydrodynamic ionization, and plasma desorption.

We have observed ions corresponding to $(M+Cl)^-$ in LD mass spectra of some amine salts. It is not known if these species arise by chloride attachment to desorbed neutrals or by fragmentation of cluster ions such as $MHCl_2^-$. Compounds like pyridoxamine also emitted abundant molecular clusters in LD. Both anionic and cationic clusters were observed. These multimers may be representative of the solid structure although clustering could also take place in the irradiated zone. Cluster-ion formation constitutes a potential source of interference when using LDMS for structural determination.

Organic salts - Considerable success has been achieved in the application of LD to analysis of organic salts. LD mass spectra of salts are characterized by high signal-to-noise ratios for salt cations (C^+) and anions (A^-). Ions arising from thermal decomposition or by dissociation of C^+ or A^- are of low abundance or undetectable at low laser power densities. This makes LDMS potentially useful for the analysis of drugs, since many are amine salts. For example, at low power density, phenisamine p-aminosalicylate gave only one major peak in the positive-ion spectrum, corresponding to the salt cation and only one peak in the negative spectrum, corresponding to the anion. At higher power densities, fragment ions and cluster species were observed. The positive ion LD mass spectrum of safranin-O, shown in Figure 6, is typical of LD results for salts. The emission of anionic species at m/z 313, though, was unusual as mentioned above.

Laser desorption of salts containing organic dications or dianions generally results in the emission of singly charged species. The LD spectrum of choline bitartrate (17) gave rise only to AH^- ions (AH_2 = tartaric acid); the tartrate dianion (A^{2-}) was not detected. LD spectra of diquarternary

dications are characterized either by abundant $[M-H]^+$ or $[M-CH_3]^+$ ions as shown in LD mass spectra of N-N'-ethylene-2,2'-bipyridyl dibromide (1) and 1,8-di(trimethyl ammonium)octane diiodide (2) in Fig. 7 (top and bottom). Peaks corresponding to fragment ions from the parent ions also could be detected for these compounds. For example, the peak at m/z 157 in the spectrum of (1) corresponds to loss of C_2H_2 from the $(M-H)^+$ ion. Similarly, the peak at m/z 199 in the spectrum of (2) corresponds to loss of CH_4 from the quasimolecular ion. We have run an extensive series of diquaternary compounds and have been unable to observe any di-positive ions. This stands in contrast to the behavior of the same compounds in SIMS.

In some cases dissociation of the doubly charged intact molecular cation (M_1^{+}, M_2^{+}) appears to occur to form M_1^{+} and M_2^{+} in the LD mass spectra. Substitution of halogens into dications can also occur. For example, the peak at m/z 298 for (2) (Fig. 7 bottom) was probably generated by the following process:

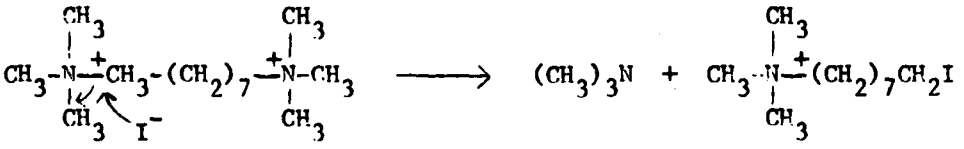

This result clearly indicates the importance of thermal processes (most likely solid-state) in the production of LD spectra.

High molecular weight compounds - Generation of quasimolecular ions of high molecular weight compounds by LD has met with mixed success. One class of compounds for which LD shows great potential is the carbohydrates. Spectra with abundant cationized molecular ions have been reported for raffinose (MW 504) and stachyose (MW 766) (17), an example of this type of

spectrum has been shown in Fig. 5-bottom. It would appear from the numbers of laboratories reporting $(M+Na)^+$ ions for sucrose that LD is the simplest and most effective method for obtaining mass spectra of oligosaccharides. Encouraging results also have been reported for polypeptides. Positive ion LD mass spectra were dominated by cationized polypeptide molecules. Very few fragment species were observed, and these were of low abundance (8). Less common but equally striking are mass spectra obtained for the glycosides digoxin (MW 780) and digitonin (MW 1228). For digoxin, $(M+Na)^+$ was emitted with about fifty percent relative abundance.

An advantage of LD as an ionization method is the generation of abundant negative ions. This is especially true for acidic substances, for which quasimolecular anions are often emitted at higher intensities than protonated or cationized species. Figure 8 shows how $(M-H)^-$ ions dominate the negative ion LD mass spectra of bile acids. This is in contrast to the positive-ion LD spectra of the bile acids which frequently show weak $(M+H)^+$ peaks or none at all· frequently only $(M+Na)^+$ peaks are observed in the positive LD spectra of these compounds.

Positive and negative ion LD spectra have been obtained for six cobalamins including the cyano, hydroxy, dimethyl methylitaconate, methyl and pereuteromethyl derivatives, along with coenzyme B_{12}. Spectra of the hydroxy derivative are shown in Figure 9. Although the quasimolecular ions are sufficient to distinguish between the derivatives, there is valuable information to be gained from the lower mass ranges as well.

The series of peaks in the m/z 400-500 mass range of the positive ion LD spectra correspond to fragments where the ribosyl phosphate and the amides on the corrin ring have been cleaved. The axial ligand which makes each cobalamin unique is not cleaved if that ligand is small. If

the axial ligands are large (as for coenzyme B_{12} and the dimethyl methylitaconate derivative) cleavage of the axial ligand just beyond the Co-C bond occurs leaving fragments in the 400-500 mass range similar to methyl cobalamin.

Polymers

Although laser pyrolysis mass spectrometry is an established technique for polymer analysis, applications of laser desorption are more recent. LD spectra of a variety of polymeric materials have shown that fingerprint mass spectra can be obtained (19). Polymers containing only carbon, hydrogen and oxygen are characterized by series of $C_nH_m^{+/-}$ peaks in their LD mass spectra. For polymers having the same backbone structure, dramatic changes in the mass spectra are observed for different side chains. For example, an abundant ion m/z 91 was observed in the positive ion LD mass spectrum of benzyl methacrylate. Phenyl methacrylate, on the other hand, is characterized by an intense phenoxide anion peak (m/z 93) in the negative ion LD mass spectrum. These are shown in Figure 10. Even for these simple polymers. analysis of LD spectra is based more on comparison with a standard than on interpretation of the unknown spectrum alone.

This is also true for more complex polymers, such as Spurr's medium, Epon 812, Biomer and Avcothane. These materials all contain more than one monomer. The structure of Biomer itself is not known. It is somewhat surprising that useful information could be obtained for these samples, but even such complex materials give fingerprint LD mass spectra. In our laboratory, LD spectra have been obtained for a polyamide and for

polydimethylsiloxane. The presence of nitrogen in the polyamide backbone and of silicon in the siloxane structure is reflected by the emission of nitrogen and silicon containing ions, respectively.

An interesting feature is seen in the negative-ion spectrum of poly-(benzylmethacrylate). The spectrum consists of a series of peaks corresponding to C_n^- and C_nH^-, and the C_nH^- peaks for n = even are nearly as intense as the C_n^- peaks, but not for n = odd. This behavior is typical of organic compounds having long aliphatic chains.

Inorganic Systems

A variety of inorganic compounds, including nonmetals, metals, metal oxides, salts, and complexes, has been examined by LDMS (10). Cluster ions $M_n^{+/-}$ are observed in LD mass spectra of C, Si, Ge, and for a number of metals. For all but carbon, cluster abundances decrease for n > 1. For carbon, C_4^- and C_6^-, and C_5^+ and C_7^+ dominate the negative and positive ion spectra, respectively. Semi-metallic elements such as Se and As show maximum abundances for Se_5^+ and As_4^+. Oxides and sulfides of As, Sb, and Bi have been examined. Ions emitted in LD are thought to be indicative of short range order of the solid.

Salts containing simple monovalent cations and anions generally yield clusters of the form $C_{n+1}A_n^+$ and $C_nA_{n+1}^-$. This is the case for sodium iodide, with clusters as large as $Na_3I_4^-$ and $Na_3I_2^+$ being observed. Higher power densities favor smaller ions. For salts with more complex ions, cluster ion formation is sometimes a minor process. Thus, for $KMnO_4$, MnO_4^- and MnO^+ are the most intense ions observed in the LD mass spectra. On

the other hand, low abundance clusters of the form C_2A^+ and CA_2^- were reported for $AgReO_4 \cdot Al(ReO_4)_4^-$ is observed for aluminum perrhenate. Extensive cluster ion emission was observed for Cu_2S. The positive ion spectrum showed CuS^+, Cu_2S^+, Cu_3S^+, $Cu_4S_2^+$ and $Cu_5S_2^+$.

A number of metal complexes has been examined by LD. In exceptional cases a molecular ion or the fully coordinated metal is observed. Complexes such as $[Co(bipy)_3](BF_4)_2$ yield $Co(bipy)_2^+$ as the highest mass ion. This is typical for chelates of bipyridyl and o-phenanthroline. In this laboratory, coordination compounds containing both amine and aminopolyacid ligands have been investigated. The aminopolyacids included iminodiacetic acid, ethylenediaminediacetic acid and EDTA. When only aminopolyacid ligands were present, ions of the form $ML_n^{+/-}$ (L = ligand) were not observed in the LD mass spectra. Often, there was no evidence in the spectrum for the presence of the ligand. Complexes containing both amine (L_1) and aminopolyacid (L_2) ligands gave ions of the form ML_1^+ and $M(L_1)_2^+$, but again the aminopolyacid ligand (L_2) did not contribute significantly to the mass spectrum.

When iodide was present as a counterion, the LD mass spectra of cobalt complexes contained abundant metal-iodide cluster ions. In some cases $Co_nI_{n-1}^+$ and $Co_nI_{n+1}^-$ dominated the mass spectra: also ions like $Co_nI_m(CN)_o^-$ were observed. A typical example of such behavior is shown for $Co(en)_3I_3$ in Figure 11. Note that formation of cluster ions occurs in both the positive- and negative-ion spectra. The two major peaks in the positive-ion spectrum correspond to Co_2CN^+ (m/z 144) and $Co(en)I^+$ (m/z 246). Note that the highest mass peak observed (m/z 619) corresponds to $Co_2(en)_2I_3^+$. The negative-ion spectrum shows only Co-I-CN combination peaks. The most intense peaks are due to

CoI_2^- and CoI_3^- (m/z 313, 440) a peak is seen at m/z 1252 corresponding to $Co_4I_8^-$. Decreasing laser power had no significant effect on the spectrum.

The analytical problem posed by interfering ions is a major one. It appears that this type of cobalt (III) complex will not give characteristic LD mass spectra when a significant amount of iodide is present. The same may be true for other metals. The appearance of cobalt-iodide clusters in LD mass spectra emphasizes the occurrence of ion-molecule reactions in the irradiated microvolume. Detailed information on these processes is not available, but they must be highly favored by kinetic or thermodynamic factors to so dominate the mass spectra.

Quantitative Analysis

The quantitative capabilities of the LAMMA 500 have not been tested rigorously. However, experiments using an epoxy resin doped with organometallic complexes of metal ions indicate that the LAMMA has high potential both in regard to reproducibility and detection limits.

Epoxy films were doped with Li, Na, Mg, K, Ca, Sr, Ba, and Pb in the concentration range between 0.1 - 1000 ppm (20). Thin sections of the doped resin (0.3 - 1 μm) were cut with an ultramicrotrome and mounted on a grid. Spectra obtained from these films indicated two things. First, the spectra were fairly reproducible from shot to shot. Second, equimolar concentrations of different metal ions gave different peak heights in the LD mass spectra. This is to be expected since the ion yields of elements vary and the ion/electron conversion efficiency at the first dynode of the detector is mass dependent. This means that application of the LAMMA to quantitative analysis will require use of elemental sensitivity factors which will have to be determined empirically for a given set of operating conditions.

Calibration curves for lead and lithium obtained using the LAMMA indicate approximate linearity over at least three decades of concentration. Although the data were plotted on a log-log scale, they represent absolute intensities and indicate reasonable reproducibility. Better reproducibility could probably be obtained using internal standard methods. The reproducibility and linearity observed show that the LAMMA is potentially a quantitative tool.

The limits of detection for various metals are summarized in Table 1. Note that both absolute and relative (concentration) detection limits are given. The absolute detection limits are quite impressive. For example, the detection limit for potassium is 1×10^{-20} gram, which corresponds to approximately 150 potassium atoms. The concentration detection limits are not as impressive ranging from 0.1 - 20 ppm. This situation occurs because the volume analyzed by the laser pulse is approximately 3×10^{-13} cm^3. Therefore, although the absolute detection limit is very high, the relative detection limit is only moderate because of the small volume sampled.

Microprobe Applications

A unique advantage of the LAMMA-500 instrument is its microprobe capability. The ability to obtain spatial information in the form of mass spectra has proved useful in a number of chemical and medical studies, several of which are mentioned here. Many of these are summarized in a recently published volume (21).

In an investigation of uranium uptake by algae, the laser microprobe gave quantitative measurements on the U content of single cells (22). The LD data were consistent with electron microprobe results. Semiquantitative analyses for Na and K in single bacterial cells were obtained and compared with measurements by atomic absorption and neutron activation (23). Figure 12 shows an electron micrograph of the irradiated cell and the mass spectrum obtained. Studies of this kind can help to elucidate the details of biochemical systems like the "sodium pump".

The spatial distribution of wood preservatives was monitored using the laser microprobe. Components of the preservatives, including boron, fluorine, chromium and copper, were detected as elemental ions (24). The authors concluded that chromium was more strongly bound to cell walls than copper. In this kind of study the speed with which data can be obtained is important. Finally, a study of Ca^{2+} in retinal tissue underscores an inherent advantage of mass spectrometric microprobes, namely, the ability to use non-radioactive isotopes for kinetic measurements (25). Calcium-44 was used to monitor the uptake of calcium by retinal tissue. Figure 13 shows the mass spectra obtained after no exposure (a), 60 minutes exposure (b), and 120 minutes exposure to a ^{44}Ca labeled solution. Clearly, the ^{44}Ca uptake is time-dependent.

Sample Handling

As is the case for other desorption ionization methods (FD, SIMS), sample preparation can be a critical factor in obtaining useful LD spectra. Usually the best spectra are obtained from solids deposited from solution on a filmed microscope grid. Water and organic solvents have

been used. For example, LD mass spectra of carbohydrates are best obtained after evaporation of a methanol solution doped with NaCl. The resulting positive ion mass spectra contain abundant $(M+Na)^+$ ions. Representative spectra (with abundant quasimolecular ions) can sometimes be obtained for crystalline organic compounds. This is not always the case: grinding the compound to a very fine powder usually improves spectral quality. LD of bile acid crystals, for instance, gave spectra with higher fragment ion abundances than when the same compound was deposited from NaCl doped ethanol. Nonetheless, an advantage of the LD methodology is that a material need not be soluble. Mass spectra can be obtained from the solid.

Ion source configuration is a factor that must be considered. In most home-built devices the laser irradiates the ion source side of the sample. The beam need not perforate the sample in this case, and large and/or thick portions of a solid can be examined. In the LAMMA-500 samples that can be perforated by the laser are preferred. Clearly, materials cannot be supported on thick (>1 μm) metal foils, and the polymer films described above must be used.

Acknowledgements

The authors would like to thank the National Science Foundation and the Office of Naval Research for support of our research in laser desorption mass spectrometry, and for funds to assist with purchase of the LAMMA-500. We also would like to thank Dr. R. Wechsung, Dr. H. Heinen, H. Vogt and L. Phillips of Leybold-Heraeus GmbH for their assistance in starting our LD research program and for their help in providing data for this paper. We also thank Professor Dr. R. Kaufman for his help and C. Parker, J. Gardella and S. Graham for helpful discussions and for data.

REFERENCES

1. Daves, G. D., Jr. Accts. Chem. Res. (1979), 12, 359-365.

2. Beckey, H. D. Int. J. Mass Spectrom. Ion Phys. (1969), 2, 500-503.

3. Mcfarlane, R. D.; McNeal, C. J. and Hunt, J. E. Adv. Mass Spectrom. (1980), 8A, 349-354.

4. Day, R. J.; Unger, S. E. and Cooks, R. G. J. Am. Chem. Soc. (1979), 101, 499-501.

5. Gardella, J. A., Jr. and Hercules, D. M. Anal. Chem. (1980), 52, 226-232.

6. Day, R. J.; Unger, S. E. and Cooks, R. G. Anal. Chem. (1980), 52, 353-354.

7. Barber, M.; Bordoli, R. S.; Sedgwick, R. D.; Tyler, A. N. J. Chem. Soc. Chem. Comm. (1981) 325-327.

8. Posthumus, M. A.; Kistemaker, P. G.; Meuzelaar, H. L. C. and Ten Noever de Brauw, M. C. Anal. Chem. (1978), 50, 985-991.

9. Conzemius, R. J. and Svec, H. J. Anal. Chem. (1978), 50, 1854-1860.

10. Conzemius, R. J. and Capellen, J. M. Int. J. Mass Spectrom. Ion Phys. (1980), 34, 197-271.

11. Nitsche, R.; Kaufmann, R.; Hillenkamp, F.; Unsöld, E.; Vogt, H. and Wechsung, R. Israel J. Chem. (1978), 17, 181-184.

12. Denoyer, E.; Van Grieken, R.; Adams, F.; Natusch, D. F. S. Anal. Chem. (1982), 54, xxx-xxx.

13. Kovalev, I. D.; Maksimov, G. A.; Suchkov, A. I. and Larkin, N. V. Int. J. Mass Spectrom. Ion Phys. (1978), 27, 101-137.

14. Cotter, R. J. Anal. Chem. (1980), 52, 1767-1770.

15. Vastola, F. J.; Pirone, A. J. Adv. Mass Spectrom. (1968), 4, 107-111.

16. Cotter, R. J. Anal. Chem. (1981), 53, 719-720.

17. Heinen, H. J.; Meier, S.; Vogt, H. and Wechsung, R. Adv. Mass Spectrom. (1980), 8A, 942-953.

18. Graham, S. W.; Dowd, P.; Hercules, D. M. Anal. Chem., submitted.

19. Cardella, J. A.; Hercules. D. M.; Heinen, H. J. Spectrosc. Letters (1980), 13, 347-360.

20. Kaufmann, R.; Hillenkamp, F.; Wechsung, R. Med. Progr. Technol. (1979), 6, 109-121.

21. Z. Anal. Chem. (1981), 308, 193-320.

22. Sprey, B.; Bochem, H.-P. Z. Anal. Chem. (1981), 308, 239-245.

23. Seydel, U.; Lindner, B. Z. Anal. Chem. (1981), 308, 253-257.

24. Klein, P.; Bauch, J. Z. Anal. Chem. (1981), 308, 283-286.

25. Schröder, W. H. Z. Anal. Chem. (1981), 308, 212-217.

Table 1

Detection Limits for Metals[a]

Metal	Absolute (g)	Relative (ppm)
Li	2×10^{-20}	0.2
Na	2×10^{-20}	0.2
Mg	4×10^{-20}	0.4
Al	2×10^{-20}	0.2
K	1×10^{-20}	0.1
Ca	1×10^{-19}	1.0
Cu	2×10^{-18}	20.0
Rb	5×10^{-20}	0.5
Cs	3×10^{-20}	0.3
Sr	5×10^{-20}	0.5
Ag	1×10^{-19}	1.0
Ba	5×10^{-19}	0.5
Pb	1×10^{-19}	0.3
U	2×10^{-19}	2.0

[a]Data provided by Leybold-Heraeus GmbH

FIGURE CAPTIONS

Figure 1. Diagram of Important Phenomena in Laser Volatilization and Ionization of Solids.

Figure 2. Time-Dependence of Laser-Induced Processes.

Figure 3. Laser Desorption Mass Spectra of Some Compounds Showing Odd-Electron Ions.

Top - Bis(dimethylamino)benzophenone-positive
Bottom - Bianthrone-negative

Figure 4. Laser Desorption Mass Spectra of Asparagine

Top - positive-ion spectrum
Bottom - negative-ion spectrum

Figure 5. Cationization Processes in Laser Desorption Mass Spectra.

Top - Glycocholic acid - positive
Bottom - Stachyose - positive (provided by Leybold-Heraeus, (GmbH))

Figure 6. Laser Desorption Positive-ion Spectrum of Safranin O.

Figure 7. Laser Desorption Mass Spectra of Doubly Charged Organic Salts

Top - N,N'-ethylene-2,2'-bipyridyl dibromide - positive
Bottom - 1,8-di(trimethyl ammonium)octane diiodide - positive

Figure 8. Negative-Ion Spectrum of Cholic Acid.

Figure 9. Laser Desorption Mass Spectra of Hydroxycobalamin.

Top - positive-ion spectrum
Bottom - negative-ion spectrum

Figure 10. Laser Desorption Mass Spectra of Polymers (19).

Top - Poly(benzylmethacrylate)
Bottom - Poly(phenylmethacrylate)

Figure 11. Laser Desorption Mass Spectra of Tris(ethylenediamine)-cobalt(III) iodide.

Top - positive-ion spectrum
Bottom - negative-ion spectrum

Figure 12. LAMMA Spectrum (right) of a Single H37 Ra-cell (left). After Seydel and Lindner (23).

Figure 13. Mass Spectra of Pigment Granules (DP).

a) control
b) 60 min incubation in ^{44}Ca solution
c) 120 min incubation in ^{44}Ca solution

After Schröder (25)

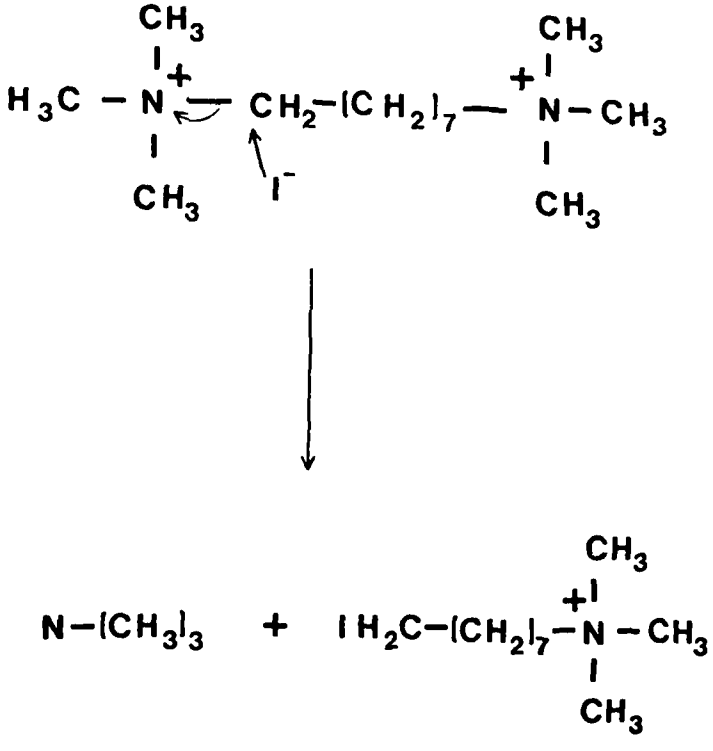

Plate for reactions

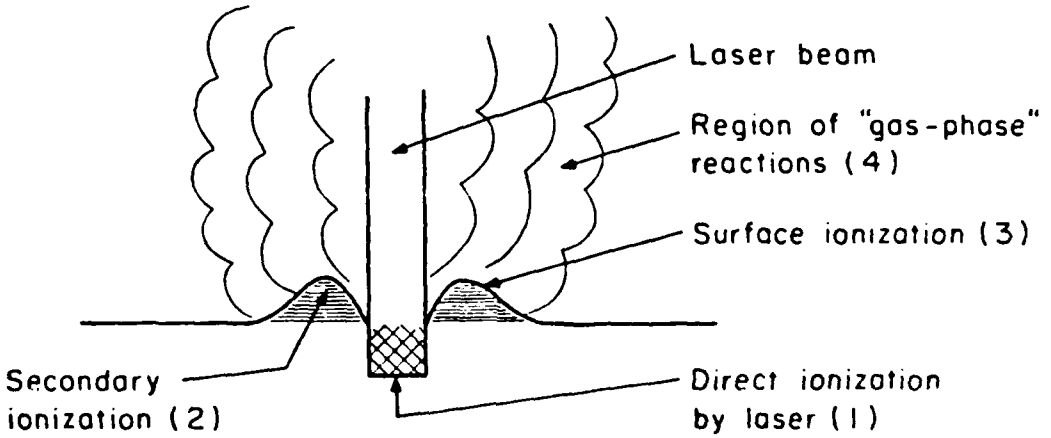
Laser beam
Region of "gas-phase" reactions (4)
Surface ionization (3)
Secondary ionization (2)
Direct ionization by laser (1)

Figure 1

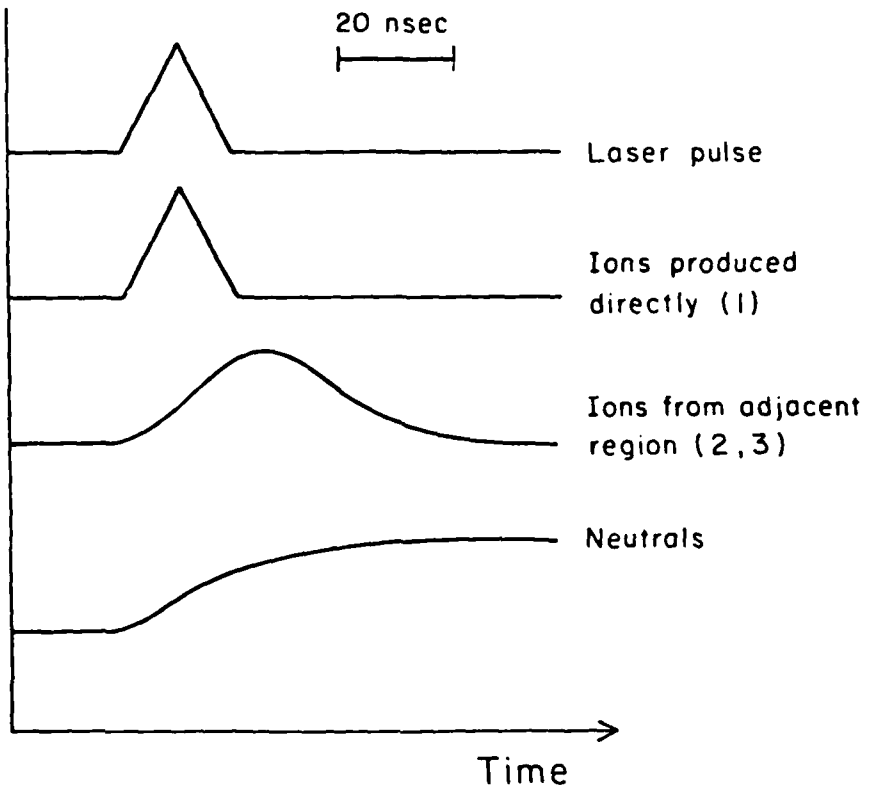
20 nsec
Laser pulse
Ions produced directly (1)
Ions from adjacent region (2,3)
Neutrals
Time

Figure 2

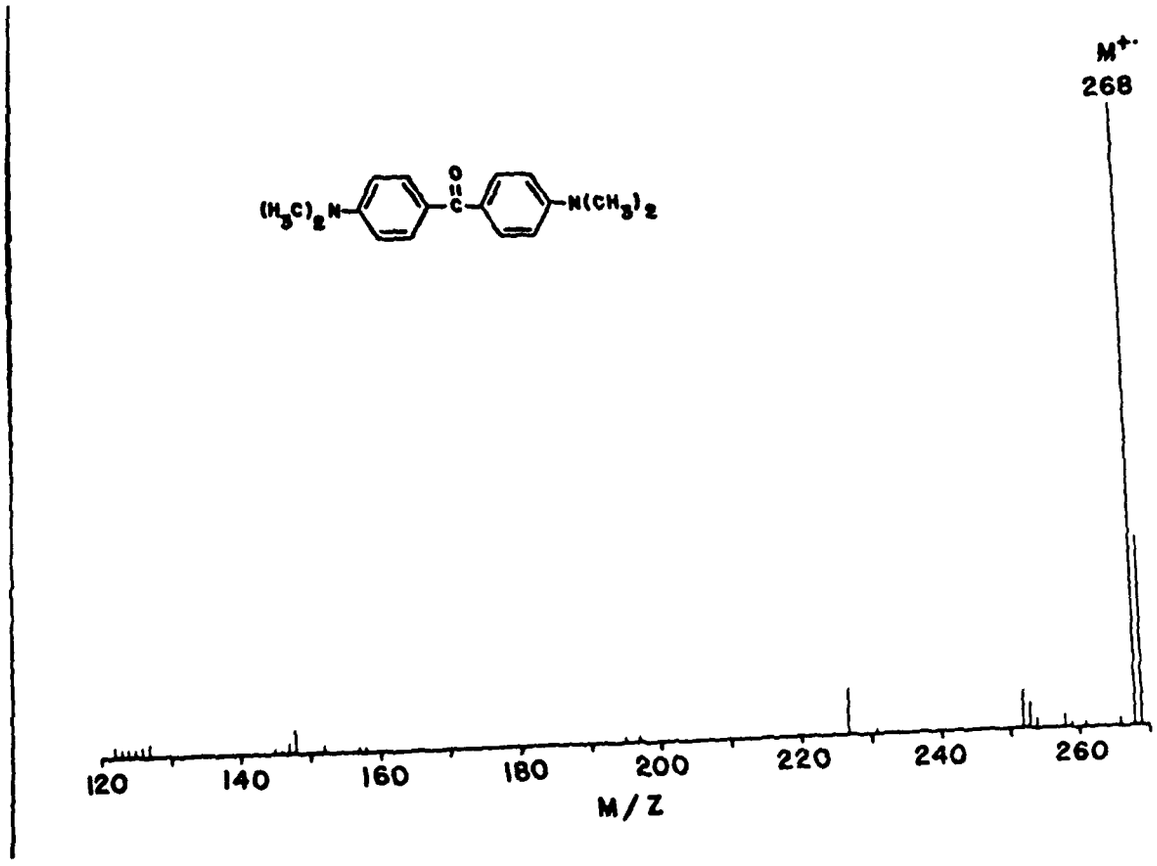

Figure 3 (top)

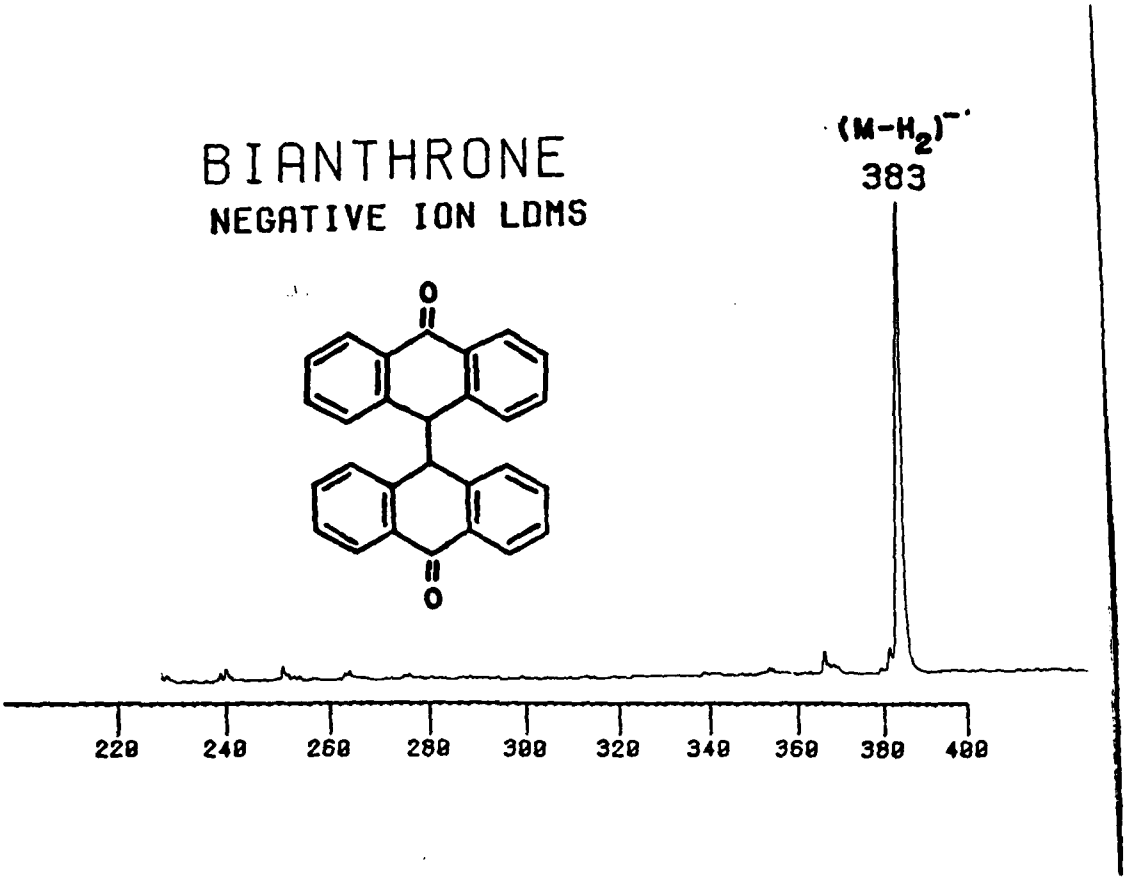

Figure 3 (bottom)

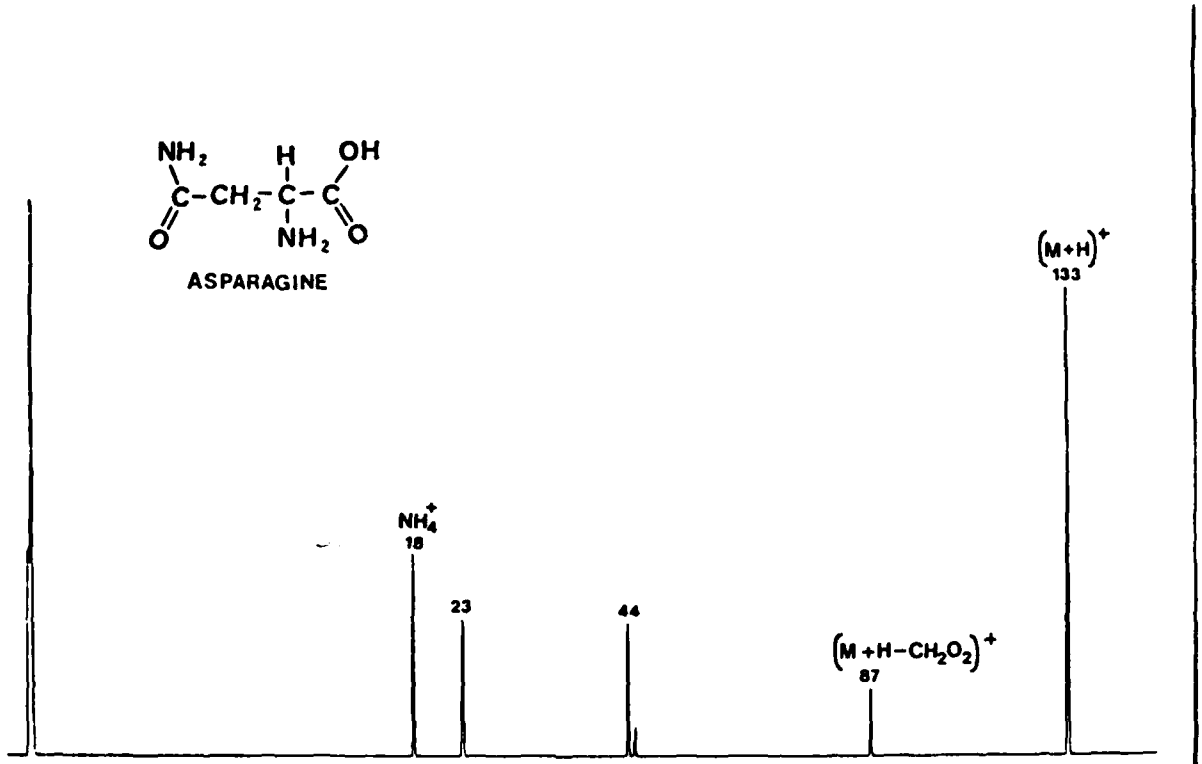

Figure 4 (top)

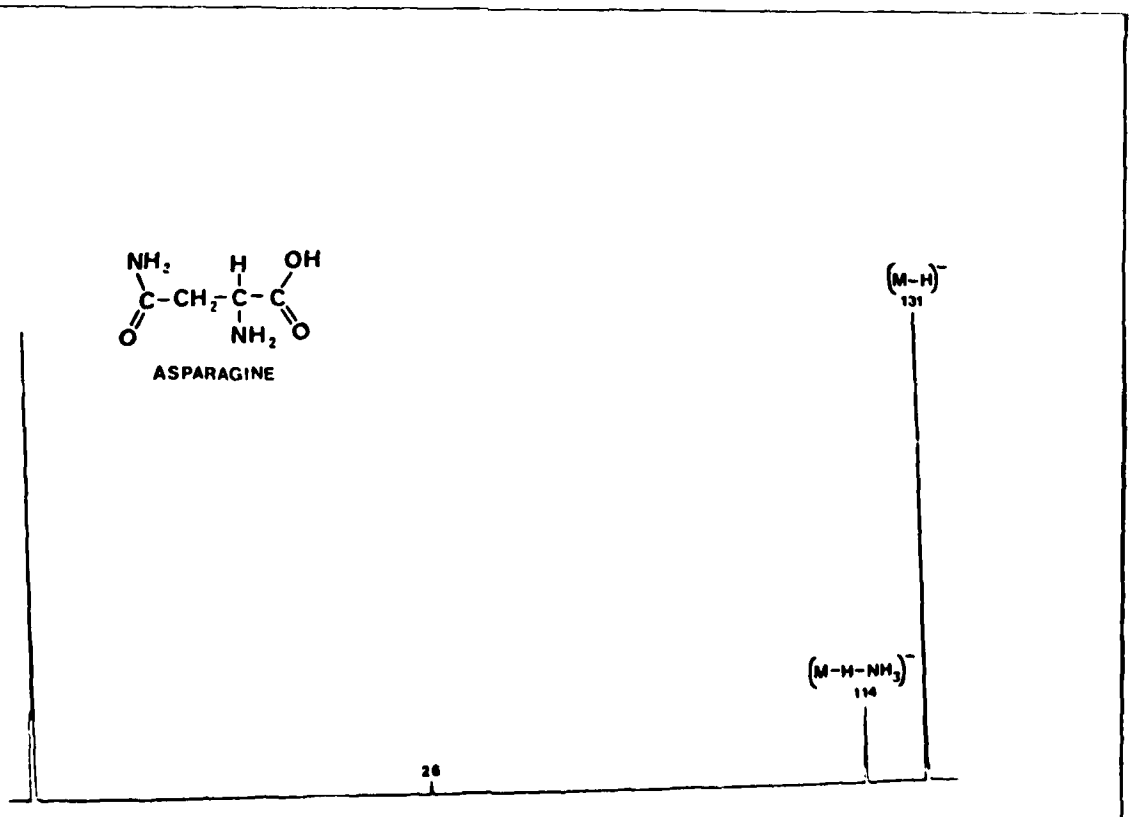

Figure 4 (bottom)

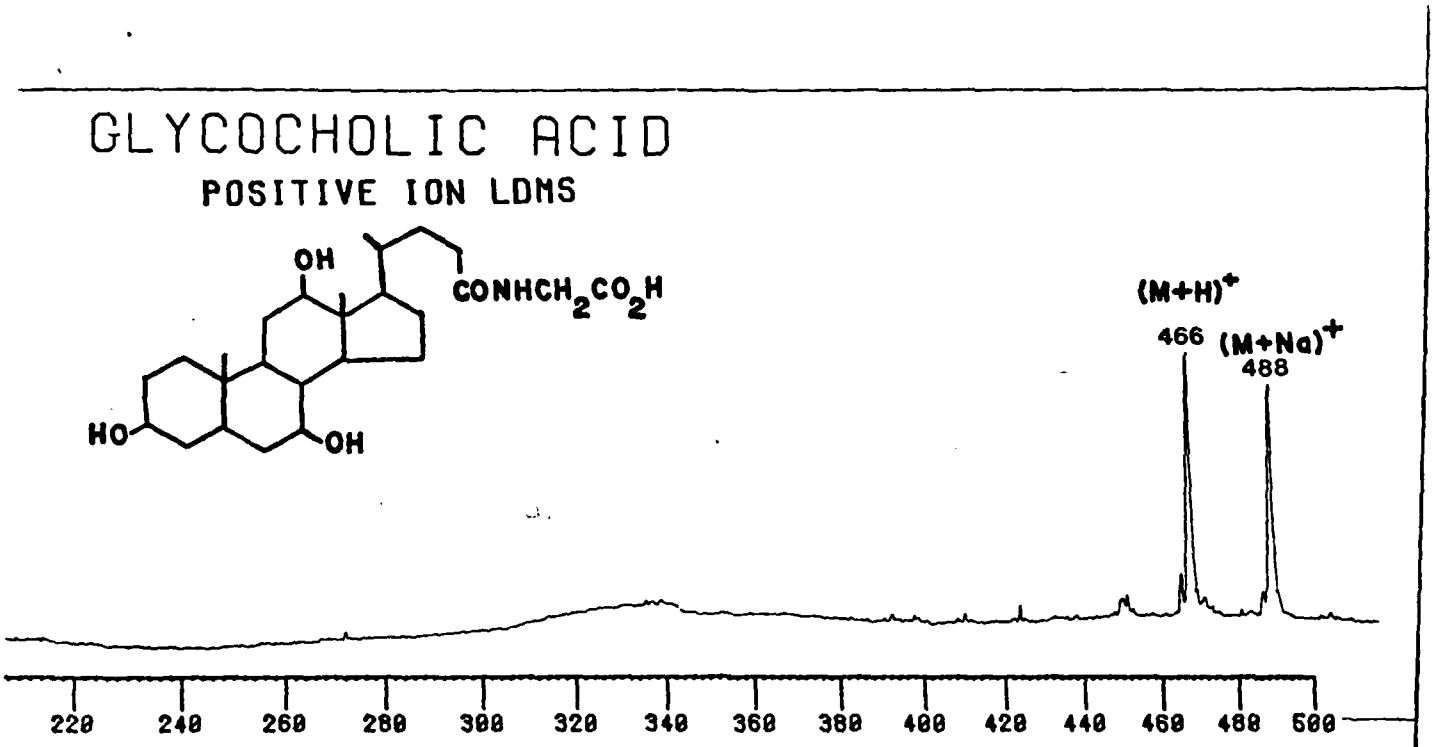

Figure 5 (top)

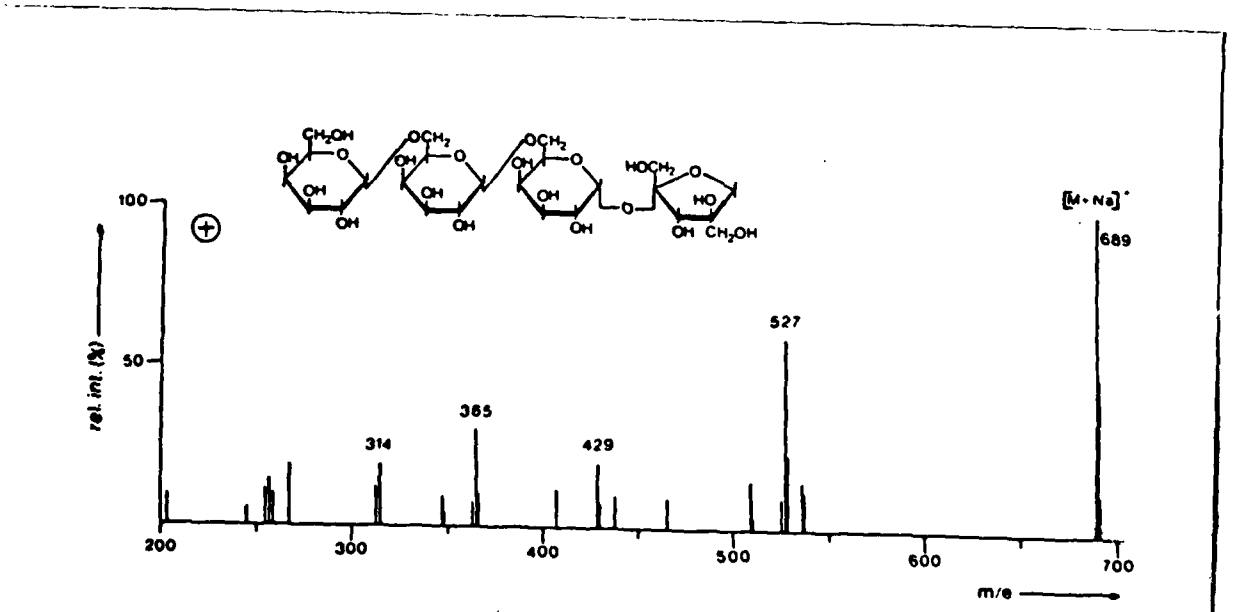

Figure 5 (bottom)

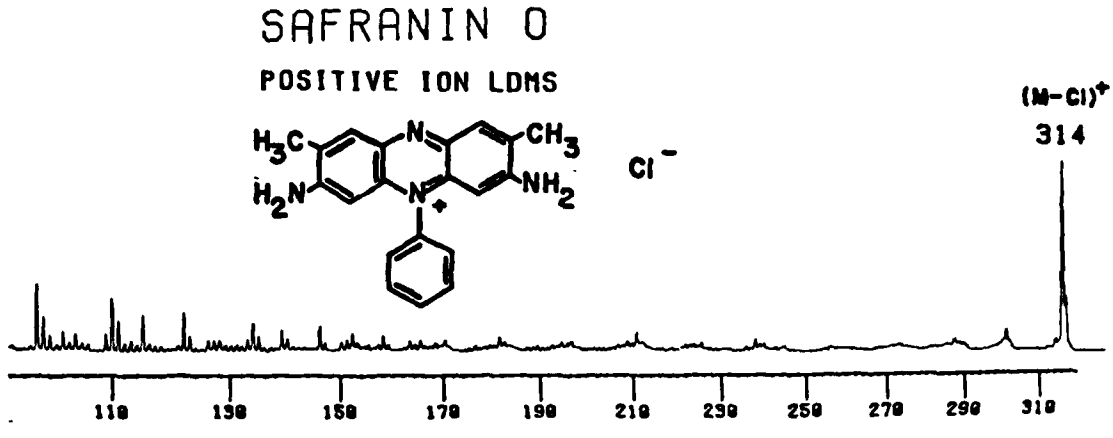
SAFRANIN O
POSITIVE ION LDMS
H_3C
CH_3
H_2N
NH_2
N
N+
Cl−
(M−Cl)+
314
110
130
150
170
190
210
230
250
270
290
310

Figure 6

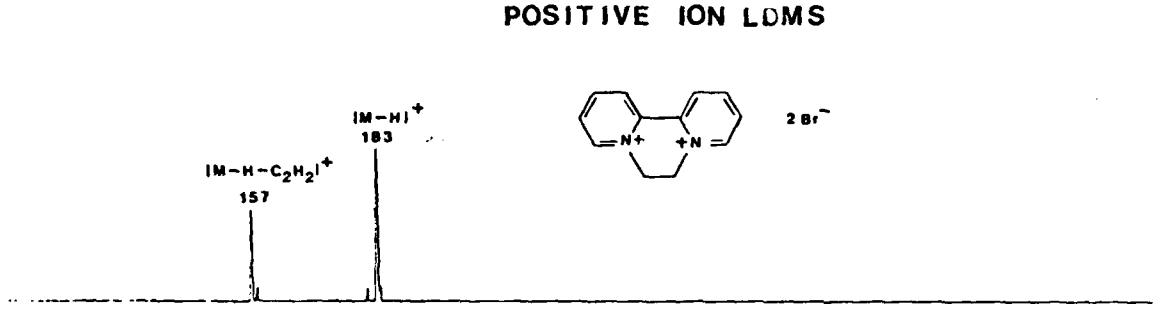

Figure 7 (top)

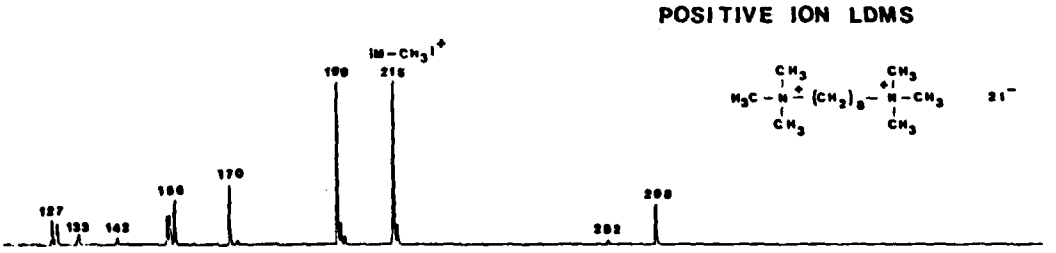

Figure 7 (bottom)

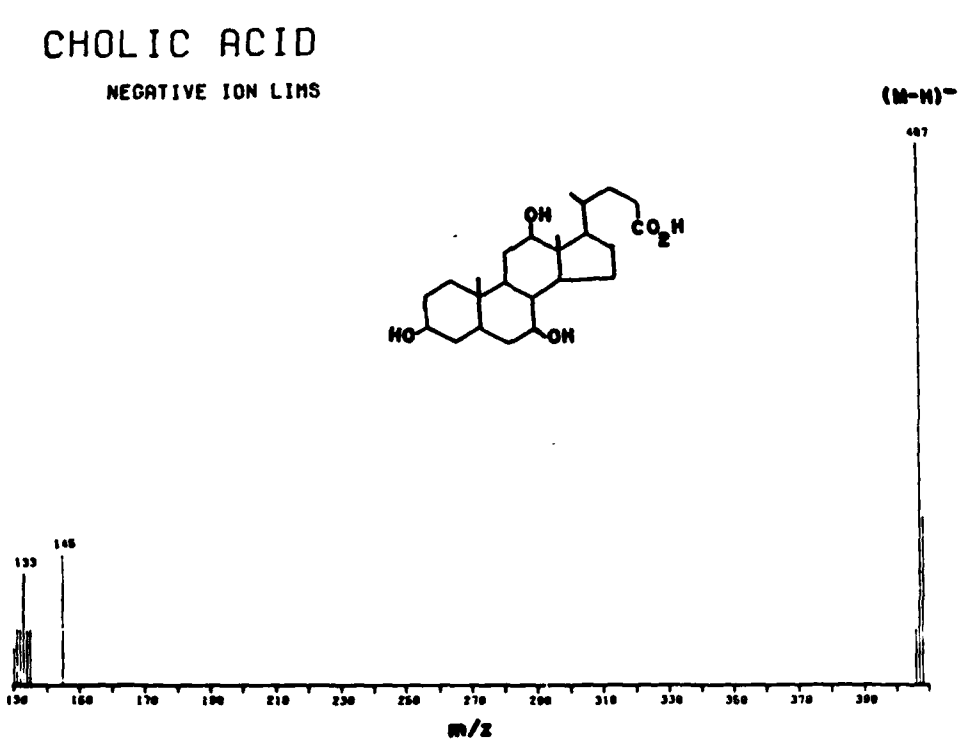
CHOLIC ACID
NEGATIVE ION LIMS
(M-H)⁻
407
OH
CO2H
HO
OH
145
133
130
150
170
190
210
230
250
270
290
310
330
350
370
390
m/z

Figure 8

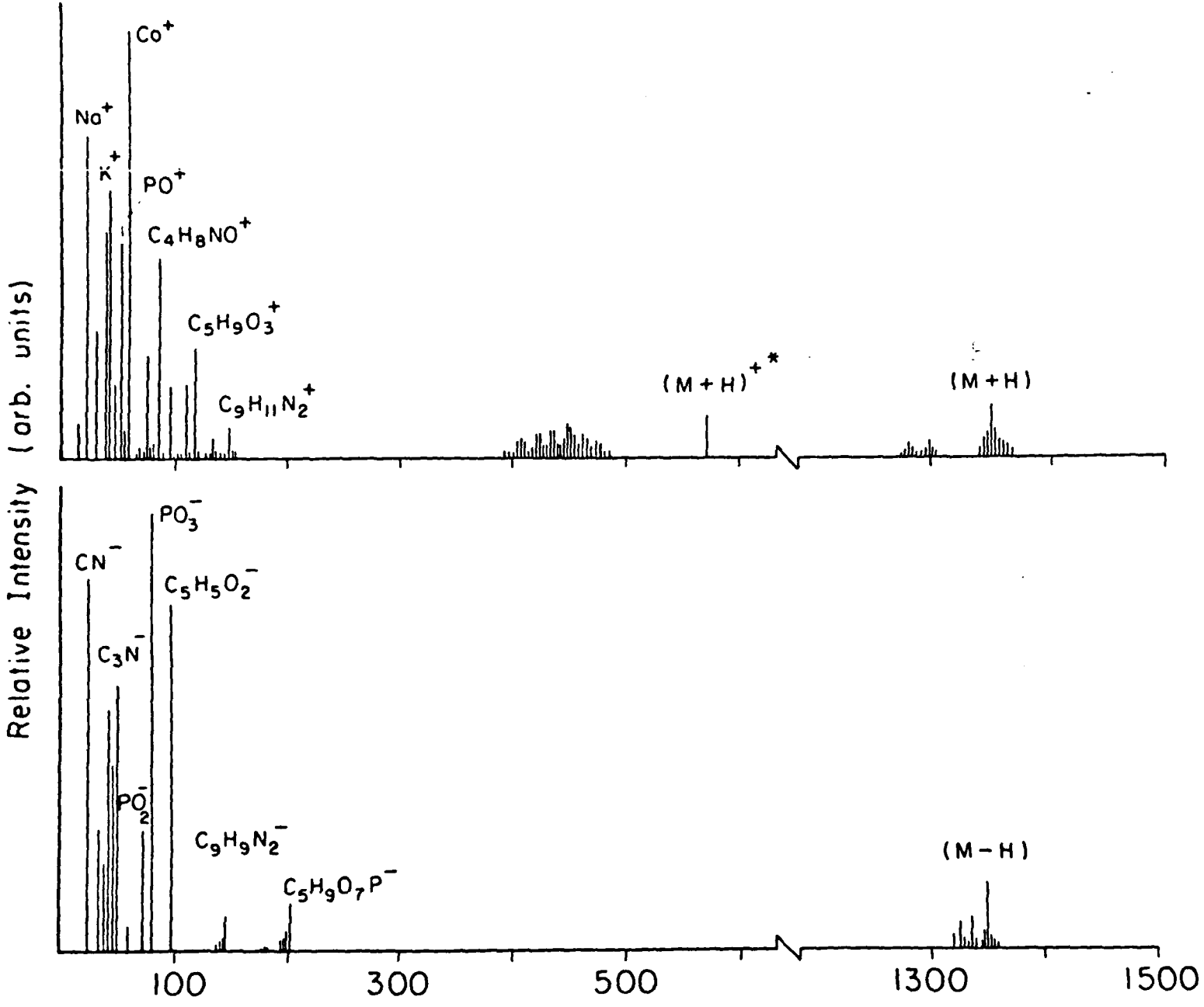
Co+
Na+
K+
PO+
C4H8NO+
C5H9O3+
C9H11N2+
(M+H)+*
(M+H)
PO3-
CN-
C5H5O2-
C3N-
PO2-
C9H9N2-
C5H9O7P-
(M-H)
Relative Intensity (arb. units)
100
300
500
1300
1500

Figure 9

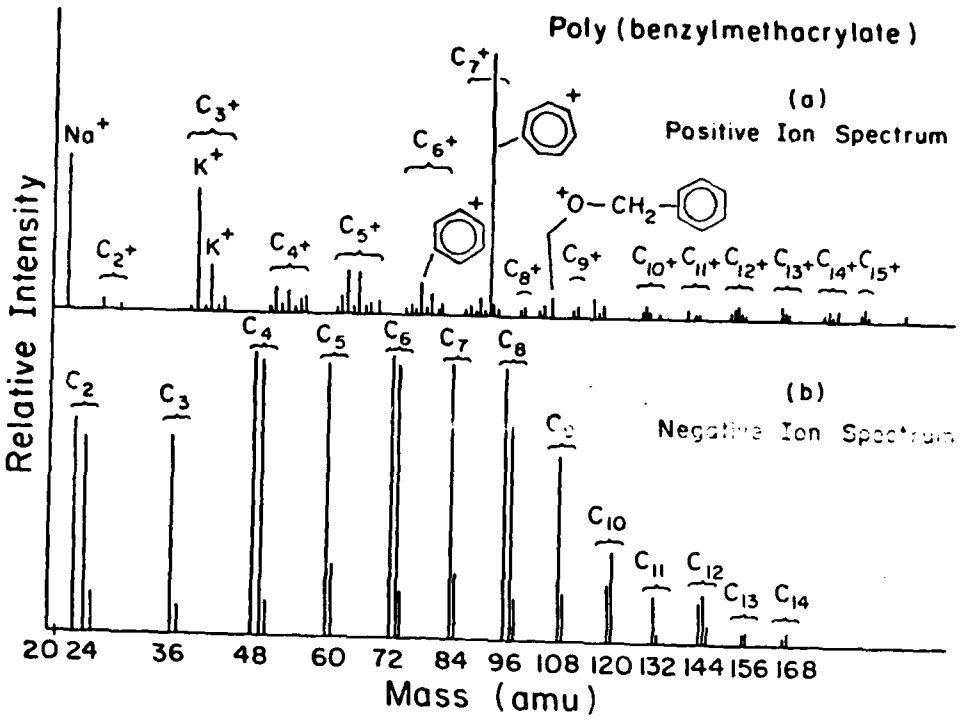

Figure 10 (top)

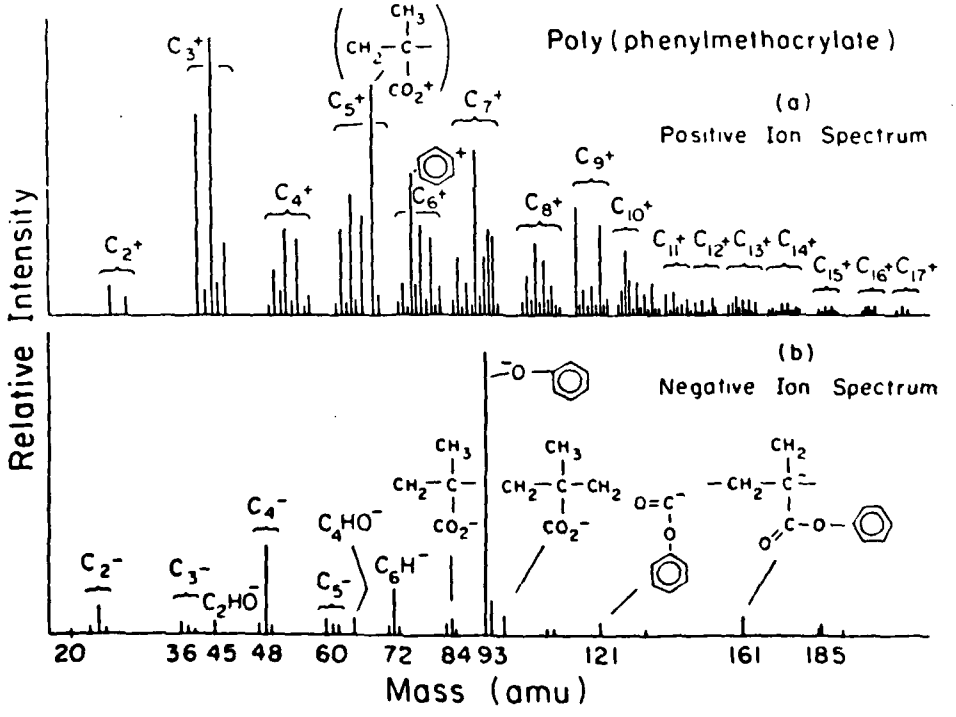

Figure 10 (bottom)

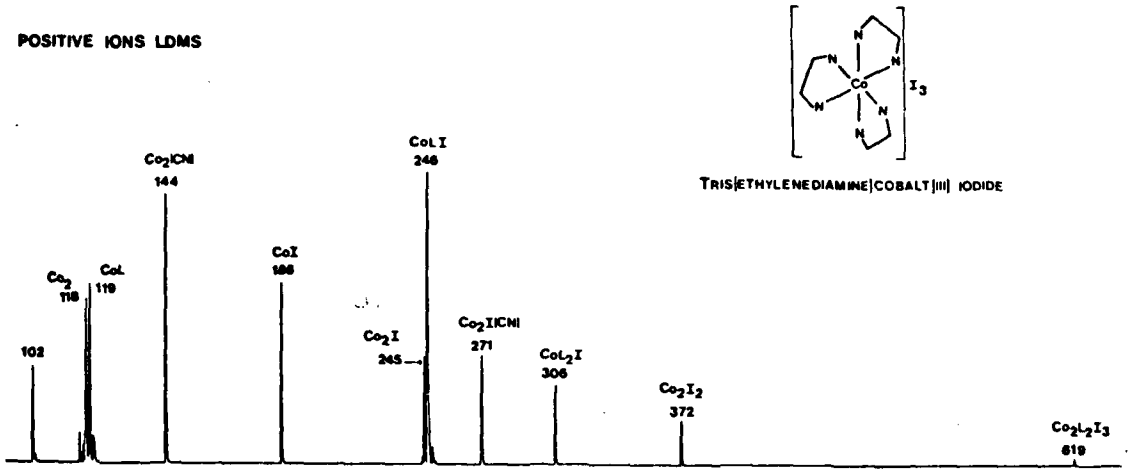

Figure 11 (top)

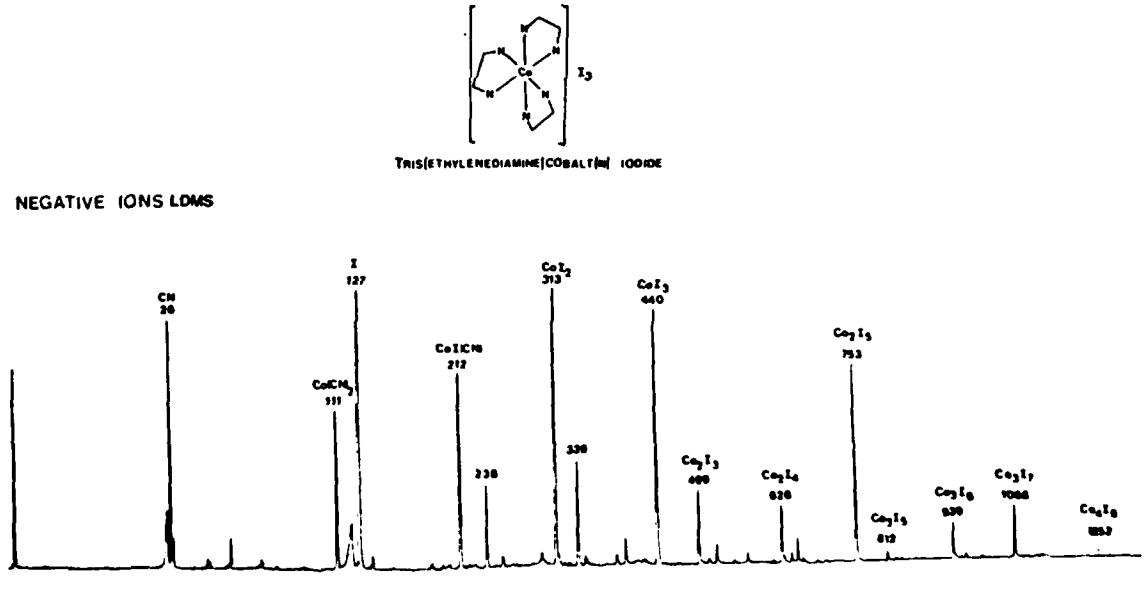

Figure 11 (bottom)

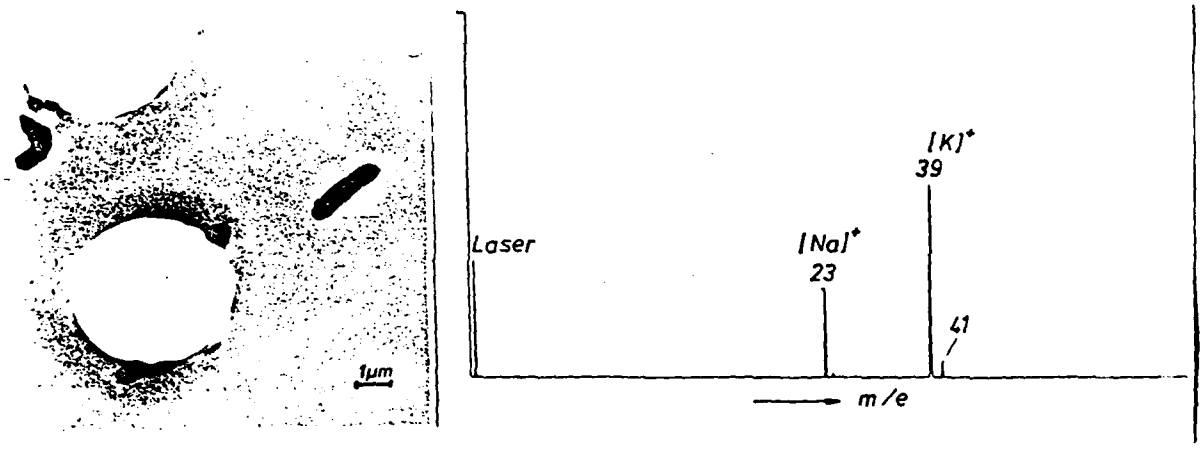

Figure 12

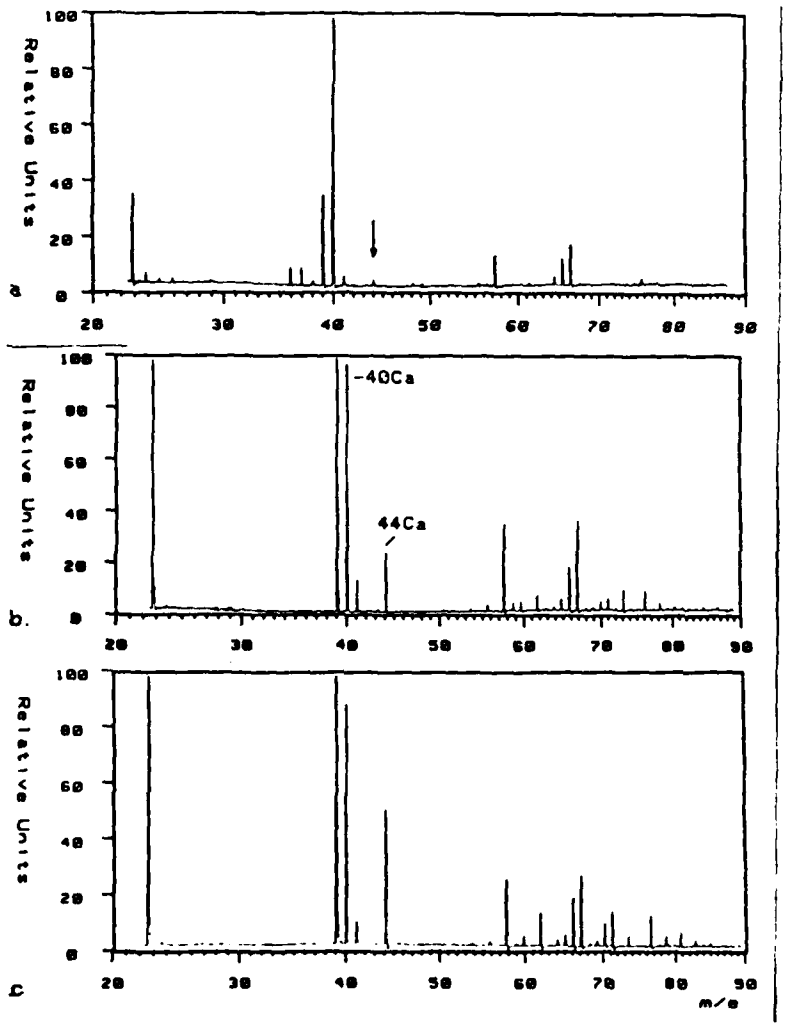
Relative Units
100
80
60
40
20
0
a
20
30
40
50
60
70
80
90
-40Ca
44Ca
b.
c
m/e

Figure 13

END

DATE
FILMED

03-82

DTIC